

# SCIENTIFIC REPORTS

OPEN

## Heterobimetallic Zeolite, InV-ZSM-5, Enables Efficient Conversion of Biomass Derived Ethanol to Renewable Hydrocarbons

Received: 21 July 2015

Accepted: 08 October 2015

Published: 03 November 2015

Chaitanya K. Narula<sup>1</sup>, Zhenglong Li<sup>1</sup>, Erik M. Casbeer<sup>1</sup>, Robert A. Geiger<sup>1</sup>, Melanie Moses-Debusk<sup>2</sup>, Martin Keller<sup>2</sup>, Michelle V. Buchanan<sup>3</sup> & Brian H. Davison<sup>2</sup>

Direct catalytic conversion of ethanol to hydrocarbon blend-stock can increase biofuels use in current vehicles beyond the ethanol blend-wall of 10–15%. Literature reports describe quantitative conversion of ethanol over zeolite catalysts but high C<sub>2</sub> hydrocarbon formation renders this approach unsuitable for commercialization. Furthermore, the prior mechanistic studies suggested that ethanol conversion involves endothermic dehydration step. Here, we report the complete conversion of ethanol to hydrocarbons over InV-ZSM-5 without added hydrogen and which produces lower C<sub>2</sub> (<13%) as compared to that over H-ZSM-5. Experiments with C<sub>2</sub>H<sub>5</sub>OD and *in situ* DRIFT suggest that most of the products come from the hydrocarbon pool type mechanism and dehydration step is not necessary. Thus, our method of direct conversion of ethanol offers a pathway to produce suitable hydrocarbon blend-stock that may be blended at a refinery to produce fuels such as gasoline, diesel, JP-8, and jet fuel, or produce commodity chemicals such as BTX.

The expansion of biomass derived ethanol industry and concurrent development of distribution channels during the last 20 years have created interest in ethanol conversion to industrial chemicals. The commercialization of ethylene derived from bioethanol represents a successful deployment of a renewable industrial chemical<sup>1,2</sup>. The addition of biomass derived ethanol to gasoline in the transportation sector is an important step in the utilization of renewable energy<sup>3</sup>. The energy independence and security act of 2007 requires 36 billion gallons of biomass derived fuel by 2022 but ethanol demand is capped at ~14 billion gallons due to “blend-wall” at 10–15%. Although a higher concentration of ethanol containing fuel (e.g., E85) has been available for several years, such fuel can be used only in flex-fuel vehicles whose U.S. market penetration is low<sup>4</sup>. This has renewed interest in the conversion of ethanol to hydrocarbon blend-stock and other industrial chemicals.

Ethanol conversion to hydrocarbons employing zeolites as catalysts dates back to 1970s<sup>5</sup>. Since then, a large number of reports have appeared in literature on ethanol conversion to hydrocarbons<sup>6–39</sup>. The reaction temperature for ethanol transformation is generally >350 °C and the pressure ranges from ambient to several atmospheres<sup>6–39</sup>. The product stream is generally high in C<sub>2</sub> hydrocarbons (e.g., ethylene and ethane), which are not valuable for liquid fuel production or commodity chemical production (separation of pure ethylene is quite expensive from a mixed stream). The mechanism of ethanol conversion

<sup>1</sup>Materials Science & Technology Division, Oak Ridge National Laboratory, Oak Ridge, TN, USA, 37831-6133.

<sup>2</sup>Energy & Environmental Sciences Directorate, Oak Ridge National Laboratory, Oak Ridge, TN 37831. <sup>3</sup>Physical Sciences Directorate, Oak Ridge National Laboratory, Oak Ridge, TN 37831. Correspondence and requests for materials should be addressed to C.K.N. (email: narulack@ornl.gov)

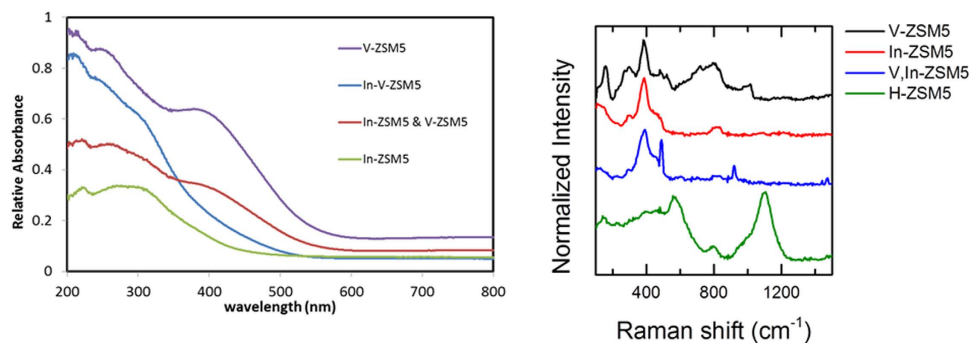


**Figure 1.** UV-Vis (left) and Raman Spectra (right) of InV-ZSM-5. For comparison, spectra of V-ZSM-5, In-ZSM-5, mechanical mixture of In-ZSM-5 and V-ZSM-5, and H-ZSM-5 are also presented.

is still being debated. A simple mechanism with ethanol dehydration to ethylene or diethyl ether as the first step and subsequent upgrading to  $C_{3+}$  hydrocarbons was proposed in 1978 by Derouane *et al.*<sup>5</sup> and reaffirmed in 2006 by Inaba *et al.*<sup>40</sup>. Recently, a hydrocarbon pool pathway for ethanol conversion has also been proposed in analogy with methanol conversion process<sup>41</sup>. A comprehensive study of decayed catalyst due to extensive coking clearly shows the presence of free radicals and their role in the ethanol transformation is being studied by Madiera *et al.* and Pinard *et al.*<sup>42–44</sup>. A recent review article summarizes state of the understanding of ethanol conversion mechanism over zeolites stating that ethanol first dehydrates to ethylene which then undergoes oligomerization to produce various olefins, paraffins, cyclics, and aromatics<sup>45</sup>. In addition, radicals provide additional active sites for secondary reactions of ethylene<sup>45</sup>. Despite these advances, the technology did not go beyond laboratory until recently<sup>46</sup> due to lack of information on optimized conversion conditions, catalyst durability, and a clear understanding of mechanism to determine energy balance of ethanol conversion.

Here, we report a versatile heterobimetallic catalyst, InV-ZSM-5, that completely converts ethanol to hydrocarbons in 250–450 °C range and atmospheric pressure without added hydrogen. The heterometallic zeolites, MM'-ZSM-5, are a new class of zeolites where the interaction between M and M' plays an important role<sup>47</sup>. The InV-ZSM-5 catalyst exhibits superior performance compared to monometallic catalysts, In-ZSM-5 or V-ZSM-5 as determined by low  $C_2$  yield and high durability. All these catalysts are robust to water content in ethanol (5–95%) and volatile impurities in fermentation stream. Furthermore, our experiments with deuterium labeling and *in situ* DRIFTS experiments rule out ethanol dehydration as a necessary step in ethanol upgrading.

## Results and Discussion

**Catalyst synthesis and characterization.** The samples of InV-ZSM-5 were synthesized by ion exchange methods. For comparison, we also prepared samples of H-ZSM-5, V-ZSM-5 and In-ZSM-5. Among these zeolites, H-ZSM-5 is the most extensively explored zeolite<sup>45</sup>. We chose V-ZSM-5 because it has been shown to be highly effective oxydehydrogenation catalyst<sup>48</sup>. For V-ZSM-5, Somorjai *et al.* pointed out that vanadium exchange leads to 95% removal of the Brønsted sites<sup>48</sup>. We expected inhibition of ethanol dehydration over V-ZSM-5 as compared with H-ZSM-5 resulting in reduced ethylene ( $C_2$ ) production. In order to increase oligomerization and aromatization, we modified V-ZSM-5 with In since In-ZSM-5 is a well-known alkane aromatization catalyst<sup>49</sup>. The In-ZSM-5 was also investigated to ensure that performance of heterobimetallic zeolite, InV-ZSM-5, is not a sum of V-ZSM-5 and In-ZSM-5. Characterization of InV-ZSM-5 is quite challenging. We have previously shown that characterization tools such as X-ray diffraction, electron microscopy, X-ray absorption near edge spectroscopy, etc., are not helpful in discerning the structure of heterobimetallic zeolites<sup>47</sup>. Hutchings *et al.* have also extensively explored the structure of bimetallic zeolites by a variety of methods<sup>50</sup>. We found that the most useful information on heterobimetallic zeolites, MM'-ZSM-5, is obtained from elemental analysis to show that both M and M' are present in MM'-ZSM-5 and UV-Vis to ascertain the presence of small clusters of M'. Finally, the reactivity is an excellent indication of the behavior of bimetallic zeolites. In our previous work, we found the activity of heterobimetallic zeolite, CuFe-ZSM-5, to be better than individual Cu-ZSM-5 or Fe-ZSM-5<sup>47</sup>. The  $C_2$  and  $C_{3+}$  selectivity of InV-ZSM-5 was superior to monometallic V-ZSM-5 or In-ZSM-5 and is described in detail in succeeding section.

A recent report suggests that Raman spectroscopy can be useful in the characterization of heterobimetallic zeolites<sup>51</sup>. Bimetallic InV-ZSM-5 used in this research has 0.6 wt% vanadium and 1.6 wt% indium, indicating both In and V are present. The UV-Vis of InV-ZSM-5 shows an absorption near 300 nm which can originate from  $In^{3+}$  and  $V^{5+}$  species since both In-ZSM-5 and V-ZSM-5 show absorption near 300 nm (Fig. 1, left). Furthermore, there is no band at 402 nm which is present in V-ZSM-5. In contrast, the mechanical mixture (V-ZSM-5 and In-ZSM-5 with V:In identical to that of InV-ZSM-5) shows

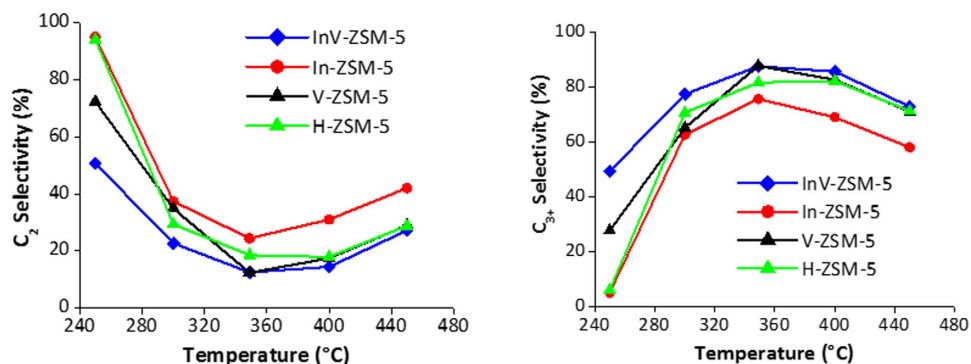


**Figure 2.** C<sub>2</sub> selectivity (left) and C<sub>3+</sub> selectivity (right) as a function of temperature for InV-ZSM-5, V-ZSM-5, In-ZSM-5 and H-ZSM-5 at WHSV of 1.6h<sup>-1</sup>.

bands at ~300 and ~400 nm. This suggests that our sample of InV-ZSM-5 is not a mechanical mixture of V-ZSM-5 and In-ZSM-5. The UV-Vis data (Fig. 1, left) on V-ZSM-5 match with literature data and exhibit vanadium bands at 286 and 402 nm which have been previously assigned to Td and Oh V<sup>5+</sup><sup>52</sup>. As reported previously, the ion exchange leads to monoionic hydroxo- or oxo-indium species at cation sites, the 300 nm absorption in UV-Vis of In-ZSM-5 can be assigned to indium species<sup>53</sup>.

The Raman spectra of our V-ZSM-5 sample (Fig. 1, right) matches with previously published Raman of V-ZSM-5 prepared from V<sub>2</sub>O<sub>5</sub> and H-ZSM-5<sup>54</sup>. The In-ZSM-5 shows strongest band at 395 cm<sup>-1</sup> with shoulders at 350 and 450 cm<sup>-1</sup>. In comparison, cubic In(OH)<sub>3</sub> exhibits bands at 137, 204, 307, 356, 390, and 659 cm<sup>-1</sup><sup>55</sup>. After crystallization to In<sub>2</sub>O<sub>3</sub> at 400 °C, bands at 125, 295, 488, and 615 cm<sup>-1</sup> are observed<sup>55</sup>. These data show that the indium species in In-ZSM-5 is not surface deposited In<sub>2</sub>O<sub>3</sub> or In(OH)<sub>3</sub>. The Raman spectrum of a mechanical mixture is identical to that of V-ZSM-5 (not shown in Fig. 1). The Raman spectrum of InV-ZSM-5, on the other hand, is very similar to that of In-ZSM-5. In addition, two sharp peaks are observed at 484 and 919 cm<sup>-1</sup>. These peaks do not match with V<sub>2</sub>O<sub>5</sub>, In<sub>2</sub>O<sub>3</sub>, or VInO<sub>4</sub>. We initially considered the possibility of these peaks due to surface adsorbed species but pretreatment involving heating to 500 °C and cooling to 200 °C in air did not change the spectrum ruling out surface adsorbed species. The additional peaks might be due to complex vanadium and indium interactions.

**Ethanol Conversion to Hydrocarbon Blend-Stock.** Ethanol conversion to hydrocarbon for all the catalysts studied is 100% in 250 °C to 450 °C range and no oxygenates are observed as shown in Fig. S1. All selectivities shown in Fig. 2 are for 100% ethanol conversion to hydrocarbons after excluding water which is 39.1% of the product stream. The InV-ZSM-5 produces much less C<sub>2</sub> than V-ZSM-5 in 250–350 °C temperature range (Fig. 2, left), however, there is no difference in C<sub>2</sub> selectivity for InV-ZSM-5 and V-ZSM-5 in 350–450 °C range. Concurrently, InV-ZSM-5 produces more valuable C<sub>3+</sub> in higher yields as compared to V-ZSM-5 in 250–350 °C and to In-ZSM-5 in 250–450 °C range. In contrast, the C<sub>2</sub> selectivity for H-ZSM-5 is higher and C<sub>3+</sub> is lower as compared to product stream from InV-ZSM-5 in 250–400 °C temperature range (Fig. 2). Thus, lower C<sub>2</sub> selectivity and higher C<sub>3+</sub> selectivity of InV-ZSM-5 over V-ZSM-5 or In-ZSM-5 in the desired temperature range makes it more desirable catalyst than monometallic ones or the un-exchanged H-ZSM-5.

The ethanol conversion reaction was run on InV-ZSM-5 after cooling the catalyst from the previous run in 250–450 °C range and the catalyst performance did not change in 250–450 °C range. This suggests that InV-ZSM-5 does not change as a result of exposure to operating conditions in 250–450 °C range. The product stream from ethanol conversion over InV-ZSM-5 contains 19% C<sub>3</sub>–C<sub>4</sub> olefins, 35% C<sub>3</sub>–C<sub>4</sub> paraffin and 33% C<sub>5+</sub> liquid fraction. The C<sub>5+</sub> liquid fraction has an average molecular weight of 97.6, average specific gravity of 0.81, and Reid Vapor Pressure of 5.14. The calculated research and motor octane numbers are 105.7 and 90.6, respectively. The liquid product stream contains over 350 compounds, consisting of 3.8% paraffins, 24.0% iso-paraffins, 6.5% olefins, 5.4% naphthenes, 60.2% aromatics, and 4.2% unidentified by volume.

**Catalyst Durability.** In view of their low C<sub>2</sub> and high C<sub>3+</sub> selectivities, the durability studies were limited to InV-ZSM-5 and V-ZSM-5 only. Gas chromatograms of hydrocarbon product streams (Fig. S2), employing 10–100% aqueous ethanol as the input stream, show that the product stream is unaffected by the fraction of water in aqueous ethanol. Regardless of the water fraction in the input stream, the ratios of individual peaks in gas chromatograms remain unchanged under our reaction conditions. Our results are different from previously reported results where water appeared to impact aromatic selectivity<sup>56</sup>. Our results suggest that fermentation streams at any stage of purification can be employed for conversion to hydrocarbon blend-stock because fermentation stream is essentially ethanol and water with small amounts of acetaldehyde, methanol, diacetyl, ethyl acetate, and acetic acid (0.1% total) even

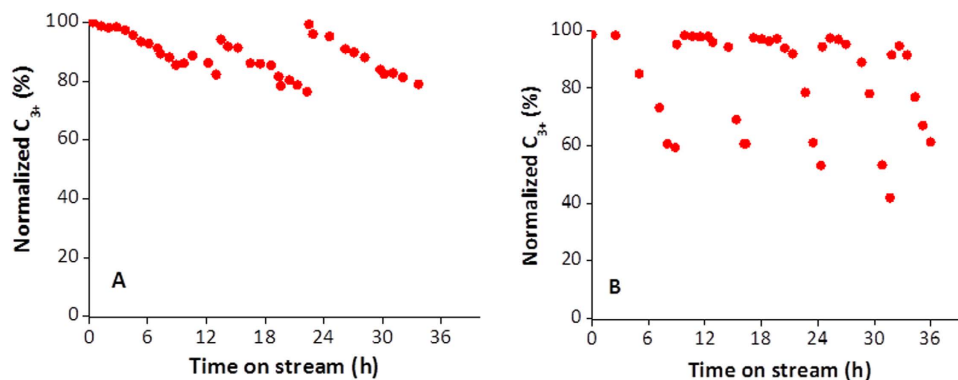


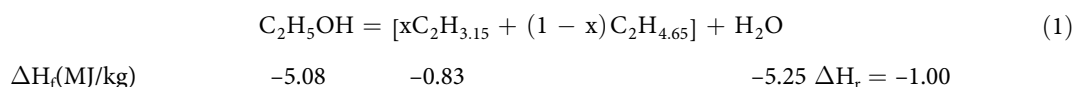
**Figure 3.** Durability tests for (left) InV-ZSM-5 and (right) V-ZSM-5 at 350°C and WHSV of 4.0 h<sup>-1</sup>.

after first flash distillation. The output stream contains C<sub>2+</sub> hydrocarbons and water which can be easily separated. A 40% ethanol solution which also contains volatile fermentation stream impurities of acetaldehyde, methanol, diacetyl, ethyl acetate, and acetic acid (0.1% total) was successfully run for 100 h over V-ZSM-5 (WHSV 1.6 h<sup>-1</sup>) with periodic decoking at 450°C. The impurities did not impact catalyst or product stream. Thus, partially concentrated ethanol stream can be used for upgrading reaction and expensive complete dewatering is not necessary.

The durability tests for InV-ZSM-5 and V-ZSM-5 were carried out at a WHSV of 4.0 h<sup>-1</sup> at 350°C employing pure ethanol (Fig. 3). The catalyst performance was monitored by the yield of C<sub>3+</sub> hydrocarbons as a function of time (normalized by the C<sub>3+</sub> yield at the beginning). The C<sub>3+</sub> yield is shown as 100% when catalyst is fresh and drops to ~80%. InV-ZSM-5 was on stream for about 12 h before C<sub>3+</sub> yield dropped below 80%. The loss in performance is due to coking, which is commonly observed in alcohol or hydrocarbon upgrading on zeolites. After decoking at 450°C, the catalyst only recovers about 94% activity because the temperature is not high enough for complete decoking to fully recover its performance. After decoking at 500°C, the catalyst fully recovers its performance. In contrast, the coking of V-ZSM-5 occurs at about 6 h at WHSV of 4.0 h<sup>-1</sup>. After decoking, the catalyst regains its performance.

Overall, InV-ZSM-5 can function twice as long as V-ZSM-5 before requiring decoking. The enhanced durability can be assigned to the incorporation of In in InV-ZSM-5. Thus, the higher C<sub>3+</sub> selectivity, described in the preceding section, and the enhanced durability of InV-ZSM-5 make it a more desirable catalyst than V-ZSM-5.

**Mechanism.** As discussed in the introduction section, there are three different proposed mechanisms for ethanol conversion to hydrocarbons – dehydration, hydrocarbon pool, and free radical. For all three pathways, the ethanol dehydration is considered to be first step. In our work, we found that ethanol conversion to hydrocarbons is exothermic ( $\Delta H_r$ , -1.0 MJ/kg) based on heat of formation data. Here, the heat of formation and chemical formula for liquid fraction were obtained experimentally. For gaseous fractions, the heat of formation data were obtained from NIST tables and the contributions of individual components were determined by GC calibrations. The value of  $x$  in equation 1 was experimentally determined to be 0.34. The overall hydrocarbon formula is slightly higher than C<sub>2</sub>H<sub>4</sub> due to error in GC yields of gaseous components.



Since ethanol dehydration is endothermic ( $\Delta H_r$  0.93 MJ/kg), the ethylene upgrading needs to be highly exothermic for overall reaction to be exothermic. The details of calculations are presented in Table S1 of supplementary section.

In order to determine if dehydration step in ethanol conversion is indeed the first step, we carried out experiments with deuterated ethanol, C<sub>2</sub>H<sub>5</sub>OD. We reasoned that deuterium will not get incorporated in the product stream if ethanol first dehydrates to ethylene or diethyl ether (Fig. S3). On the other hand, if ethanol conversion does not involve dehydration, product stream will contain deuterated hydrocarbons. Our results show that the conversion of C<sub>2</sub>H<sub>5</sub>OD or a mixture of 70% C<sub>2</sub>H<sub>5</sub>OH and 30% D<sub>2</sub>O results in deuterium incorporation in all hydrocarbons in the product stream including ethane except in ethylene. A likely explanation for deuterium incorporation is that hydrocarbon pool mechanism is a pathway for ethanol conversion to C<sub>2+</sub> hydrocarbons and C<sub>2</sub>H<sub>5</sub>OD adds and eliminates across C=C containing organics (aliphatic or side chain on aromatics) inside zeolites resulting in deuterium incorporation.

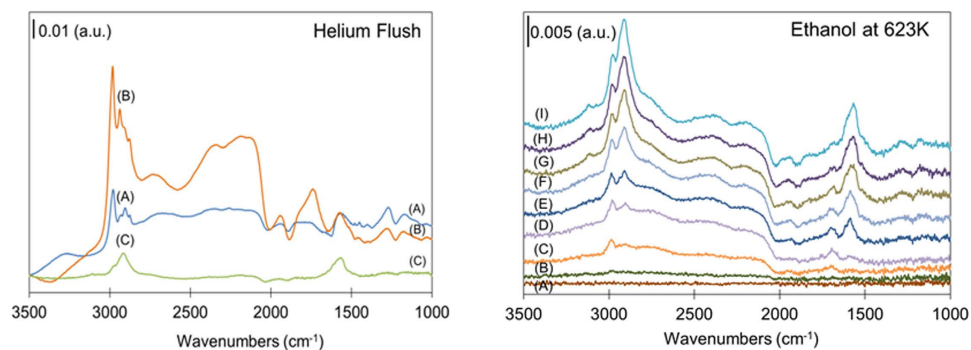


**Figure 4.** *In-situ* DRIFT absorbance spectra of samples exposed to ethanol and after flushing with helium for 10 minutes samples at (A) 25 °C, (B) 200 °C, and (C) 350 °C (left) and at 350 °C as a function of ethanol exposure time after (A) no exposure (B) 0.1 min; (C) 0.2 min; (D) 0.5 min; (E) 1.3 min; (F) 2.9 min; (G) 5.0 min; (H) 6.9 min; (I) 10.0 min (right).

The deuterium exchange of catalyst hydroxyl group as a pathway for deuterium incorporation in product stream could be easily ruled out since the product stream from catalytic conversion of a mixture of 70%  $C_2H_4$  and 30%  $D_2O$  did not show any deuterium incorporation. The cation in the catalyst also does not play a role in deuterium incorporation because, regardless of the cations (H or V) in the catalyst, the deuterium incorporation was seen in product streams when either  $C_2H_5OD$  or a mixture of 70%  $C_2H_5OH$  and 30%  $D_2O$  are employed as reactants and no deuterium incorporation is observed in the product stream from a mixture of 70%  $C_2H_4$  and 30%  $D_2O$ .

The energy balance and deuteration experiments can be explained if we consider initiation, propagation, and termination steps of ethanol conversion individually. It is possible that initial hydrocarbon pool forms from ethylene via dehydration step but the formation of initial hydrocarbon pool from ethoxy groups cannot be ruled out. As such, we show both possibilities in Fig. S4. It is also quite challenging to determine if ethylene in the product stream is from dehydration or hydrocarbon pool. However, the conventional dehydration mechanism can be definitely ruled out based on deuterium labeling experiment. The propagation can occur via hydrocarbon pool pathway since free radical pathway does not allow for deuterium incorporation in the product stream. The hydrocarbon pool pathway allows for deuterium incorporation since ethanol can directly add to  $-C=C-$  in both olefin and aromatic cycles. After ethanol addition, the loss of water can occur with either deuterium or hydrogen on carbon adjacent to ethoxy group (Fig. S4). The termination of reaction occurs with gradual transformation of hydrocarbon pool into coke. This is supported by gradual increase in ethylene formation and decrease in  $C_3$  and higher hydrocarbon yields. The coking has been observed previously and decoking restores catalyst activity.

The support for propagation via hydrocarbon pool pathway also comes from our diffuse reflectance infra-red studies into progress of ethanol upgrading over V-ZSM-5 (Fig. 4). Figure 4A compares the spectra after the samples had been flushed with helium for 10 min to clean the cell of gas phase products and unreacted ethanol. A low intensity, broad band around  $3263\text{ cm}^{-1}$  was observed during the 25 °C study which can be attributed the O-H stretch of an alcohol. The absence of this band in either the 200 or 350 °C studies indicates that all ethanol adsorbed on the catalyst has reacted at these elevated temperatures which is consistent with experimental observation that all ethanol is converted to products at 200 °C or above. The C-H of the alkyl groups is present at all temperatures in the  $2700\text{--}3000\text{ cm}^{-1}$  region and at  $\sim 1570\text{ cm}^{-1}$ , respectively<sup>57</sup>. The presence of C-H and C=C stretches at 350 °C is consistent with experimental observation of formation of non-oxygenated hydrocarbon species. Our results match very well with those reported recently by Sousa *et al.*<sup>58</sup> and essentially show that at temperature below 350 °C, ethoxy, diethyl ether, and ethylene species are present which are not observed above 350 °C.

We also carried out additional experiments to monitor changes in DRIFTS as a function of time after initial ethanol adsorption. A series of spectra, showing the changes that occur on the catalyst during the first 10 min, were captured immediately before and during the exposure of fresh V-ZSM-5 to ethanol flow at 350 °C (Fig. 4B). In the first 0.5 min of ethanol flow, before the C=C band of alkylated aromatics at  $1567\text{ cm}^{-1}$  band appears, a band at  $1690\text{ cm}^{-1}$  can be detected which may indicate the presence of linear alkenes. The band at  $1567\text{ cm}^{-1}$  is not the dominant band in this region until  $\sim 1.3$  min, after which the intensity of the band increases with time while that of  $1690\text{ cm}^{-1}$  band decreases. The proposal of an initial alkene formation followed quickly by the formation of aromatics on the zeolite surface is further supported by the changes in the C-H stretching region. The absorption at  $2987\text{ cm}^{-1}$  is the dominant C-H stretching band immediately after exposure to ethanol, while the  $2911\text{ cm}^{-1}$  becomes dominant after roughly 3 min. The  $2987\text{ cm}^{-1}$  does not diminish like  $1690\text{ cm}^{-1}$  but increases at a slower rate than  $2911\text{ cm}^{-1}$  and is red shifted from its original frequency to  $2978\text{ cm}^{-1}$ <sup>59,60</sup>. This may indicate that the position of the alkenes is no longer on the catalyst, but as substituents on the aromatics. These data

suggest that linear alkene form at the initiation of reaction but aromatics become dominant within first minutes.

Thus, we have shown that heterobimetallic zeolite InV-ZSM-5 is more effective and durable in converting ethanol to liquid hydrocarbons. Our work with deuterium labeling does not conclusively prove any of the three proposed pathways in literature but supports hydrocarbon pool pathway and creates doubt about dehydration being the necessary first step.

## Methods

**Catalysts Synthesis.** Commercial  $\text{NH}_4$ -ZSM-5 (CBV2314) was purchased from Zeolyst Corporation. H-ZSM-5 was prepared by thermal treatment of commercial  $\text{NH}_4$ -ZSM-5 at 500 °C for 4 h. V-ZSM-5 was prepared by a modification of a literature method<sup>61</sup>.  $\text{NH}_4$ -ZSM-5 ( $\text{SiO}_2/\text{Al}_2\text{O}_3 = 23$ ) was soaked in V(III)  $\text{Cl}_3$  aqueous solution. Specifically, a 0.05 M solution of V(III)  $\text{Cl}_3$  was first made by dissolving 2.5 g of V(III)  $\text{Cl}_3$  into 320 mL of distilled water. Then, 12.17 g of  $\text{NH}_4$ -ZSM-5 was added to the aqueous solution and warmed to 80 °C. After stirring for 16 hours under reflux condition, the mixture was vacuum filtered, and the solid was dried at 105 °C overnight. The light blue V-ZSM-5 solid was then calcined at 500 °C for four hours, which resulted in a light yellow final catalyst. In-ZSM-5 was synthesized using similar method as V-ZSM-5. Indium (III) nitrate was used as the precursor. For bimetallic InV-ZSM-5 preparation, V-ZSM-5 was first prepared with same V loading. Indium (III) nitrate aqueous solution of 0.015 M was prepared. V-ZSM-5 was then ion-changed with indium nitrate solution under reflux condition for 16 hours at 80 °C. After filtration, washing and drying at 105 °C, the catalyst was calcined at 500 °C for four hours with 1 °C/min ramping rate.

**Elemental Analysis.** Elemental analyses were performed by Galbraith Incorporated, Knoxville, TN. V-ZSM-5 has about 0.7 wt% vanadium loading. Indium loading in In-ZSM-5 was 1.6 wt%. Bimetallic InV-ZSM-5 has 0.6 wt% vanadium and 1.6 wt% indium.

**UV-Vis-NIR and Raman analyses.** Diffuse reflectance UV-Vis spectra were collected on a Cary 5000 UV-Vis-NIR spectrophotometer under R% mode. Raman spectroscopy was performed with an Alpha 300 confocal micro-Raman setup (WITec Inc., Germany) using a 532 nm excitation laser with a 20X objective and 600 g/mm (grooves per millimeter) grating. The laser power was attenuated to 300 uW and the laser spot size was approximately 1  $\mu\text{m}$ .

***In-situ* diffuse reflectance FT infrared spectroscopy (DRIFTS) analysis.** *In-situ* diffuse reflectance FT infrared spectroscopy (DRIFTS) measurements were performed on a Nicolet Nexus 670 spectrometer equipped with a MCT detector cooled by liquid nitrogen, and an *in-situ* chamber (HC-900, Pike Technologies) with capability to heat samples to 1173 K. The exiting stream was analyzed by an online quadrupole mass spectrometer (QMS) (OmniStar GSD-301 O2, Pfeiffer Vacuum). All samples studied by DRIFTS were heated to desired testing temperatures (room temperature (RT), 473 and 623 K) under a flow of 50 sccm of 100% helium and held at this temperature for at least 10 min before exposure to ethanol. A DRIFT spectrum of each fresh sample was taken at the desired testing temperature to confirm no IR active species were present before ethanol testing began. Ethanol reactant gas was created by injecting ethanol using a syringe pump at a rate of 0.04 mL/h into a heated flow of 50 sccm helium. Space velocity conditions were kept constant from sample to sample. A series of spectra were captured to monitor the changes in absorbance on the catalyst surface as a function of time upon exposure to the ethanol flow.

**Catalytic conversion of ethanol.** A quartz reactor (8 mm ID  $\times$  25 cm H) was loaded with 0.2 g of catalyst (250–500  $\mu\text{m}$ ) between two layers of quartz wool. Two thermocouples were used to measure the temperatures, one in the middle of catalyst bed to measure catalyst temperature and the other one right below the quartz wool to measure the inlet gas temperature. All the reported temperatures in this paper are inlet gas temperature unless otherwise stated. The catalyst temperatures are similar for different catalysts at same inlet gas temperature. A tubular furnace was used to heat the catalyst up to 450 °C and hold for 0.5 h under 50 sccm dry helium flow. Then we changed it to catalyst testing temperatures and waited until the temperature stabilized. Pure ethanol (unless otherwise stated) was fed into the reactor employing a syringe pump. After stabilizing for 0.5 h, product analysis was performed by an on-line gas chromatograph (Agilent 6850) and mass spectrometer (5975C MS). The transfer line between the reactor and the GC/MS was heated to around 250 °C to prevent condensation of heavy products. Capillary column, HP-Plot Q, was used, with a dimension of 30.0 m  $\times$  320  $\mu\text{m}$   $\times$  20.0  $\mu\text{m}$ . GC was held at 50 °C for 3 min, ramped up to 250 °C at 15 °C/min and then held for 35 min. Constant pressure mode of 9.51 psi was used and the inlet temperature was 250 °C. A gas calibration mixture (1% ethylene, 1% propene, 1% isobutene, 1% isopentane and balance nitrogen) was used to calibrate  $\text{C}_2$  to  $\text{C}_5$  hydrocarbons. Standards of benzene, toluene, p-xylene, ethylbenzene and cumene were used to quantify aromatic compounds. Nitrogen (5 sccm) was used as internal standard for all the analyses. For durability test, catalyst was regenerated under 20 ccm air flow with temperature ramped up to 450 °C at 2 °C/min, holding for 15 min, then ramping up to 500 °C and holding for 1 h.

**Liquid Hydrocarbon Analysis.** The liquid product stream was collected in a liquid nitrogen trap. A sample of the liquid product stream was exposed to ambient temperature and pressure to allow evaporation of low-boiling products to allow for safe transportation. The sample was separated from water, dried over anhydrous  $\text{MgSO}_4$ , and sent to SGS Oil, Gas, and Chemicals, Deer Park, TX 77536 for analysis (referred to as SGS analysis in the paper).

**Deuterium Labeling Experiments.** A set of experiments involved employing deuterated ethanol. The rationale was that deuterium will not get incorporated if ethanol first dehydrates to ethylene or diethyl ether (Fig. S3). All these experiments were carried out in the quartz tube reactor (mentioned above). Products identification was performed using online GC/MS.

## References

1. Le Van Mao, R., Levesque, P., McLaughlin, G. & Dao, L. H. Ethylene from ethanol over zeolite catalysts. *Appl. Catal.* **34**, 163–179 (1987).
2. Green Products. Available at: <http://www.braskem.com.br/site.aspx/green-products-USA> (Accessed: September 30, 2015)
3. Regulation for fuels and fuel additives: 2012 renewable fuel standards, 40 CFR Part 80 [EPA-HQ-OAR-2010-0133; FRL-9614-4]. Available at: <http://www.gpo.gov/fdsys/pkg/FR-2012-01-09/pdf/2011-33451.pdf> (Accessed: September 30, 2015).
4. Conti, J. J. *et al.* Annual energy outlook 2015 with projections to 2040, U.S. Energy Information Administration. Report Number: DOE/EIA-0383 (2015). Available at: [http://www.eia.gov/forecasts/aeo/pdf/0383\(2015\).pdf](http://www.eia.gov/forecasts/aeo/pdf/0383(2015).pdf) (Accessed: September 30, 2015)
5. Derouane, E. G. *et al.* Elucidation of the mechanism of conversion of methanol and ethanol to hydrocarbons on a new type of synthetic zeolite. *J. Catal.* **53**, 40–55 (1978).
6. Aguayo, A. T., Gayubo, A. G., Tarrío, A. M., Atutxa, A. & Bilbao, J. Study of operating variables in the transformation of aqueous ethanol into hydrocarbons on a HZSM-5 zeolite. *J. Chem. Technol. Biotechnol.* **77**, 211–216 (2002).
7. Whitcraft, D. R., Verykios, X. E. & Mutharasan, R. Recovery of ethanol from fermentation broths by catalytic conversion to gasoline. *Ind. Eng. Chem. Process Des. Dev.* **22**, 452–458 (1983).
8. Aldridge, G. A., Verykios, X. E. & Mutharasan, R. Recovery of ethanol from fermentation broths by catalytic conversion to gasoline. 2. Energy analysis. *Ind. Eng. Chem. Process Des. Dev.*, **23**, 733–738 (1984).
9. Aguayo, A. T., Gayubo, A. G., Atutxa, A., Valle, B. & Bilbao, J. Regeneration of a HZSM-5 zeolite catalyst deactivated in the transformation of aqueous ethanol into hydrocarbons. *Catal. Today* **107–108**, 410–416 (2005).
10. Schulz, J. & Bandermann, F. Conversion of ethanol over metal-exchanged zeolites. *Chem. Eng. Technol.* **16**, 332–337 (1993).
11. Marques, J. P. *et al.* Infrared spectroscopic study of the acid properties of dealuminated BEA zeolites. *Microporous Mesoporous Mater.* **60**, 251–262 (2003).
12. Saha, S. K. & Sivasanker, S. The conversion of ethanol to hydrocarbons over ZSM-5. *Indian J. Technol.* **30**, 71–76 (1992).
13. Gayubo, A. G., Alonso, A., Valle, B., Aguayo, A. T. & Bilbao, J. Selective production of olefins from bioethanol on H-ZSM-5 zeolite catalysts treated with NaOH. *Appl. Catal. B: Environmental* **97**, 299–306 (2010).
14. Makarfi, Y. *et al.* Conversion of bioethanol over zeolites. *Chem. Eng. J.* **154**, 396–400 (2009).
15. Madeira, F. F., Gnepp, N. S., Magnoux, P., Maury, S. & Cadran, N. Ethanol transformation over HFAU, HBEA, and HMFI zeolites presenting similar Bronstead acidity. *Appl. Catal. A* **367**, 39–46 (2009).
16. Inoue, T. *et al.* Synthesis of LEV zeolite by interzeolite conversion method and its catalytic performance in ethanol to olefins reaction. *Microporous Mesoporous Mater.* **122**, 149–154 (2009).
17. Gujar, A. C. *et al.* Reactions of methanol and higher alcohols over H-ZSM-5. *Appl. Catal. A* **363**, 115–121 (2009).
18. Calsavara, V., Baesso, M. L. & Fernandes-Machado, N. R. C. Transformation of ethanol into hydrocarbons on ZSM-5 zeolites modified with ion in different ways. *Fuel* **87**, 1628–1636 (2008).
19. Inaba, M., Murata, K. & Takahara, I. Effects of Fe-loading and reaction temperature on the production of olefins from ethanol by Fe/H-ZSM-5 zeolite catalysts. *React. Kinet. Catal. Lett.* **97**, 19–26 (2009).
20. Ouyang, J., Kong, F., Su, G., Hu, Y. & Song, Q. Catalytic conversion of bio-ethanol to ethylene over La-modified HZSM-5 catalysts in a bioreactor. *Catal. Lett.* **132**, 64–74 (2009).
21. Pinard, L. *et al.* Growth mechanism of coke on HBEA zeolite during ethanol transformation. *J. Catal.* **299**, 284–297 (2013).
22. Wang, F., Luo, M., Xiao, W., Cheng, X. & Long, Y. Coking behaviour of a submicron MFI catalyst during ethanol dehydration to ethylene in a pilot-scale fixed-bed reactor. *Appl. Catal. A* **393**, 161–170 (2011).
23. Inaba, M., Murata, K., Takahara, I. & Inoue, K. Production of olefins from ethanol by Fe and/or P-modified H-ZSM-5 zeolite catalysts. *J. Chem. Technol. Biotechnol.* **86**, 95–104 (2011).
24. Song, Z., Takahashi, A., Nakamura, I. & Fujitani, T. Phosphorous-modified ZSM-5 for conversion of ethanol to propylene. *Appl. Catal. A* **384**, 201–205 (2010).
25. Goto, D. *et al.* Conversion of ethanol to propylene over HZSM-5 type zeolites containing alkaline earth metals. *Appl. Catal. A* **383**, 89–95 (2010).
26. Xia, W. *et al.* Study of active sites on the MFI zeolite catalyst for the transformation of ethanol into propylene. *J. Mol. Catal. A* **328**, 114–118 (2010).
27. Bi, J., Guo, X., Liu, M. & Wang, X. High effective dehydration of bio-ethanol into ethylene over nanoscale HZSM-5 zeolite catalysts. *Catal. Today* **149**, 143–147 (2010).
28. Gayubo, A. G., Alonso, A., Valle, B., Aguayo, A. T. & Bilbao, J. Selective production of olefins from bioethanol on hzsm-5 zeolite catalysts treated with NaOH. *Appl. Catal. B: Environmental* **97**, 299–306 (2010).
29. Ivanova, S. *et al.* Binderless HZSM-5 coating on  $\beta$ -SiC for different alcohols dehydration. *Appl. Catal. A* **359**, 151–157 (2009).
30. Zhu, Q., J. Kondo, J. N., Inagaki, S. & Tatsumi, T. Catalytic activities of alcohol transformations over 8-ring zeolites. *Top. Catal.* **52**, 1272–1280 (2009).
31. Song, Z., Takahashi, A., Mimura, N. & Fujitani, T. Production of propylene from ethanol over ZSM-5 zeolites. *Catal. Lett.* **131**, 364–369 (2009).
32. Makarfi, Y. I. *et al.* Conversion of bioethanol over zeolites. *Chem. Eng. J.* **154**, 396–400 (2009).
33. Tsuchida, T., Yoshioka, T., Sakuma, S., Takeguchi, T. & Ueda, W. Synthesis of biogasoline from ethanol over hydroxyapatite catalyst. *Ind. Eng. Chem. Res.* **47**, 1443–1452 (2008).
34. Inaba, M., Murata, K., Saito, M. & Takahara, I. Production of olefins from ethanol by Fe-supported zeolite catalysts. *Green Chem.* **2007**, 9, 638.
35. Aguayo, A. T., Gayubo, A. G., Tarrío, A. M., Atutxa, A. & Bilbao, J. Study of operating variables in the transformation of aqueous ethanol into hydrocarbons on a HZSM-5 zeolite. *J. Chem. Technol. Biotechnol.* **77**, 211–216 (2002).
36. Ramaswamy, K. K., Zhang, H., Sun, J. M. & Wang, Y. Conversion of ethanol to hydrocarbons on hierarchical HZSM-5 zeolites. *Catal. Today* **238**, 103–110 (2014).

37. Ramaswamy, K. K. & Wang, Y. Ethanol conversion to hydrocarbons on HZSM-5: Effect of reaction conditions and Si/Al ratio on the product distribution. *Catal. Today* **237**, 89–99 (2014).
38. Nieskens, D. L. S., Ferrar, D., Liu, Y. & DePutter, S. A. Effects of oxygenate impurities on the conversion of alcohols to olefins. *Ind. & Eng. Chem. Res.* **53**, 10892–10898 (2014).
39. Lethaeghe, D., van der Mynsbrugge, J., Vandichel, M. & van Speybroeck, V. Full theoretical cycle for both ethane and propene formation during methanol-to-olefin conversion in H-ZSM-5. *ChemCatChem* **3**, 208–212 (2011).
40. Inaba, M., Murata, K., Saito, M. & Takahara, I. Ethanol conversion to aromatic hydrocarbons over several zeolite catalysts. *React. Kinet. Catal. Lett.* **88**, 135–141 (2006).
41. Johansson, R., Hruby, S. L., R.-Hansen, J. & Christensen, C. H. The hydrocarbon pool in ethanol-to-gasoline over HZSM-5 catalysts. *Catal. Lett.* **127**, 1–6 (2009).
42. Madeira, F. F. *et al.* Radical species detection and their nature evolution with catalyst deactivation in the ethanol-to-hydrocarbon reaction over HZSM-5 Zeolite. *ACS Catal.* **1**, 417–424 (2011)
43. Pinard, L. *et al.* On the involvement of radical “coke” in ethanol conversion to hydrocarbons over HZSM-5 zeolite. *Catal. Today* **218–219**, 57–64 (2013).
44. Ben Tayeb, K. *et al.* Ethanol transformation into higher hydrocarbons over HZSM-5 zeolite: direct detection of radical species by *in situ* EPR spectroscopy. *Catal. Comm.* **27**, 119–123 (2012).
45. Sun, J. & Wang, Y. Recent advances in catalytic conversion of ethanol to chemicals. *ACS Catal.* **4**, 1078–1090 (2014).
46. Vertimass licenses ORNL bio-fuel-to-hydrocarbon conversion technology. Available at <http://www.vertimass.com/news.php> (Accessed: September 30, 2015).
47. Yang, X. *et al.* Heterometal incorporation in metal-exchanged zeolites enables low-temperature catalytic activity of NO<sub>x</sub> reduction. *J. Phys. Chem. C* **116**, 23322–23331 (2012).
48. Chang, Y.-F., Somorjai, G. A. & Heinemann, H. Oxydehydrogenation of ethane over ZSM-5 zeolite catalysts. *Appl. Catal. A* **96**, 305–318 (1993).
49. Halez, J. *et al.* Structural properties and catalytic activity in selective oxidation of In-containing ZSM-5 catalysts. *J. Mol. Structure* **651–653**, 315–322 (2003).
50. Hammond, C. *et al.* Elucidation and evolution of the active component within Cu/Fe/ZSM-5 for catalytic methane oxidation: from synthesis to catalysis, *ACS Catal.* **3**, 689–699 (2013).
51. Xia, H., Fleischman, S. D., Li, C. & Scott, S. L. Spectroscopic evidence of extra-framework heterometallic oxo-clusters in Fe/Ga-ZSM-5 catalysts. *J. Phys. Chem. Lett.* **2**, 190–195 (2011).
52. Sen, T., Rajamohanam, P. R., Ganapathy, S. & Sivasanker, S. The nature of vanadium in vanado-silicate (MFI) molecular sieves: influence of synthesis methods. *J. Catal.* **163**, 354–364 (1996).
53. Schmidt, C., Sowade, T., Loeffler, E., Birkner, A. & Gruenert, W. Preparation and structure of In-ZSM-5 catalysts for the selective reduction of NO by hydrocarbons. *J. Phys. Chem. B* **106**, 4085–4097 (2002).
54. Lacheen, H. S. & Iglesia, E. Synthesis, structure, and catalytic reactivity of isolated V<sup>3+</sup>-oxo species prepared by sublimation of VOCl<sub>3</sub> onto H-ZSM-5. *J. Phys. Chem. B* **110**, 5462–5472 (2006).
55. Yang, J., Frost, R. L. & Martens, W. N. Thermogravimetric analysis and hot-stage Raman spectroscopy of cubic indium hydroxide. *J. Therm. Anal. Calorim.* **100**, 109–116 (2010).
56. Oudejans, J. C., Van Den Oosterkamp, P. F. & Van Bekkum, H. Conversion of ethanol over zeolite H-ZSM-5 in the presence of water. *Appl. Catal.* **3**, 109–115 (1982).
57. Hemelsoet, K., Ghysels, A., Mores, D., De Wispelaere, K. & Van Speybroeck, V. Experimental and theoretical IR study of methanol and ethanol conversion over H-SAPO-34. *Catal. Today* **177**, 12–24 (2011).
58. Sousa, Z. S. B., Cesar, D. V., Henriques, C. A. & deSilva, V. T. Bioethanol conversion into hydrocarbons on HZSM-5 and HMC-22 zeolites: use of *in situ* DRIFTS to elucidate the role of the acidity and of the pore structure over the coke formation and product distribution. *Catal. Today* **234**, 182–191 (2014).
59. Pinard, L. *et al.* Growth mechanism of coke on HBEA zeolite during ethanol transformation. *J. Catal.* **299**, 284–297 (2013).
60. Douberly, G. E., Ricks, A. M., Schleyer, P.v.R. & Duncan, M. A. Infrared spectroscopy of gas phase benzenium ions: protonated benzene and protonated toluene, from 750 to 3400 cm<sup>-1</sup>. *J. Phys. Chem. A* **112**, 4869–4874 (2008).
61. Wark, M., Koch, M., Bruckner, A. & Grunert, W. Investigation of zeolites by photoelectron and ion scattering spectroscopy Part IV XPS studies of vanadium-modified zeolites. *J. Chem. Soc., Faraday Trans.* **94**, 2033–2041 (1998).

## Acknowledgements

This research is sponsored by the U.S. Department of Energy, Office of Energy Efficiency and Renewable Energy, BioEnergy Technologies Office under contract DE-AC05-00OR22725 with UT-Battelle, LLC. Initial funds were from the ORNL Laboratory Directed Research and Development funds and from the BioEnergy Science Center which is supported by the U.S. DOE Office of Biological and Environmental Research in the Office of Science. The DRIFTS work was performed at the Center for Nanophase Materials Sciences, which is sponsored at Oak Ridge National Laboratory by the Scientific User Facilities Division, Office of Basic Energy Sciences, and U.S. Department of Energy. We thank Dr. Zili Wu for help with DRIFTS experiments and Mr. Andrew Lepore for assistance with some of the experimental work. Authors thank Drs. Jagjit Nanda and Rose Ruther for recording Raman spectra of zeolites.

## Author Contributions

All authors reviewed the manuscript and have given approval to the final version of the manuscript. The original concept and progression of this work evolved from multiple discussions between C.N., B.D. and M.K. C.N. did primary writing with assistance of B.D., Z.L., R.G., E.C. and Z.L. are post-doctoral associates who did the experimental work and prepared figures under the direction of C.N. The experimental work included the preparation of the catalysts, the operation of the reactor and the analysis. M.D. carried out DRIFTS work. MB reviewed the results and suggested experiments with ethanol and D<sub>2</sub>O to confirm the alternative mechanism.

## Additional Information

**Supplementary information** accompanies this paper at <http://www.nature.com/srep>

**Competing financial interests:** ZL, EC, RG, MD, and MB declare no competing financial interests. CN, BH, and MK own stock in Vertimass, LLC, licensee of the technology described in this report.

**How to cite this article:** Narula, C. K. *et al.* Heterobimetallic Zeolite, InV-ZSM-5, Enables Efficient Conversion of Biomass Derived Ethanol to Renewable Hydrocarbons. *Sci. Rep.* **5**, 16039; doi: 10.1038/srep16039 (2015).



This work is licensed under a Creative Commons Attribution 4.0 International License. The images or other third party material in this article are included in the article's Creative Commons license, unless indicated otherwise in the credit line; if the material is not included under the Creative Commons license, users will need to obtain permission from the license holder to reproduce the material. To view a copy of this license, visit <http://creativecommons.org/licenses/by/4.0/>